I&EC research
Industrial & Engineering Chemistry Research

Article

pubs.acs.org/IECR

Intracrystalline Mesoporosity over Y Zeolites: PASCA Evaluation of the Secondary Cracking Inhibition in the Catalytic Cracking of Hydrocarbons

Juan Rafael García, Marisa Falco, and Ulises Sedran*

Instituto de Investigaciones en Catálisis y Petroquímica (INCAPE), UNL-CONICET, Colectora Ruta Nac. 168 Km 0 (3000) Santa Fe, Argentina

ABSTRACT: Two FCC catalyst prototypes were prepared using Y zeolite with different intracrystalline mesoporosity, which were used in the cracking of *n*-hexadecane (batch fluidized bed reactor, reaction time 4 s, temperatures 500 and 550 °C, catalyst/reactant 2.6). The primary and secondary cracking analysis method (PASCA), based on balances of carbon atoms among cracking products, showed that increasing the mesoporosity in Y zeolite decreases the incidence of secondary cracking as compared to primary cracking, thus increasing the selectivity to intermediate products. This positive effect was the consequence of the improvements in the diffusion transport of primary product molecules which, in diffusing faster out of the pores, have fewer chances to suffer further cracking. The experiments at different temperatures, with both the prototypes and the equilibrium commercial FCC catalysts, confirmed that this method is a simple tool that allows characterizing the cracking performance of FCC catalysts under conditions similar to those in commercial plants.

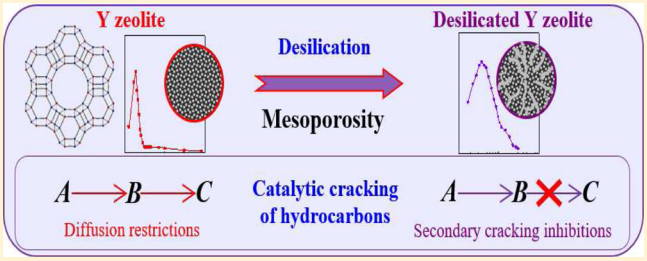

1. INTRODUCTION

The worldwide driving forces for innovations in the process of catalytic cracking of hydrocarbons (FCC), which is a mature process in refineries, aimed at producing transportation fuels as well as petrochemical raw materials, include both the increasing demands for diesel fuel and particularly propylene and the rising use of various residual feedstocks.[1−3] Residues differ from standard hydrocarbon FCC feedstocks, which are typically vacuum gas oils (VGO), in their higher contents of contaminant metals, polynuclear aromatics, heteroatoms, and complex macromolecular groups.[4]

Commercial FCC catalysts are composed by Y zeolite crystals supported on a matrix, which can be either active or inactive; binder, filler, and additives with different roles are also included in the catalysts.[2,5] The particle size of the catalysts is about 70 μm on average, the zeolite crystals being smaller than 1 μm.[5,6] FCC being a catalytic process, it is necessary that reactant molecules diffuse in this porous system in order to reach the active sites, which are located in the zeolite micropore structure, adsorb and react. Then chemical (mainly acidity) and textural properties have a controlling impact on the performance of these catalysts.[7] Bulky molecules with critical diameters larger than the micropore size in Y zeolite (7.4 Å), which are typical in FCC feedstocks, would hardly access internal sites due to serious diffusion restrictions in the pore system.[6−12]

Diffusion restrictions in porous catalysts where complex reactions take place (the case of FCC) can impact not only on the observed catalyst activity but also on the selectivities to the various products.[13−15] For example, the higher the restrictions on the primary products in consecutive reactions, the lower their observed selectivities.[13,14,16,17] Thus, improvements in the transport properties of the commercial FCC catalysts would be attractive because the selectivity to desired intermediate products could be increased and undesired secondary reactions could be attenuated.[8,11−14] This is particularly true for the case of diesel fuel, whose blend is contributed by the light cycle oil (LCO) cut from FCC, which, in a very simplified view, can be understood as an intermediate product in the overall conversion scheme.

Other secondary reactions, such as hydrogen transfer, will be conditioned by diffusion transport limitations, and consequently, any improvement in transport will impact negatively on their relative importance. Hydrogen transfer reactions are considered to play an important role among the large number of complex reactions that occur in the FCC process, since they have a strong impact on product quality, mainly on gasoline octanes, and catalyst stability.[5]

Among the various strategies which have been postulated to moderate the negative impact of diffusion restrictions in Y zeolite,[7,10,16,17] the use of smaller crystals providing shorter diffusion paths has been extensively studied.[9,15] A different approach is the generation of intracrystalline mesoporosity by means of desilication treatments.[8,10−12] The treatment comprises an alkaline leaching, which selectively removes silicon atoms from the crystalline network, thus inducing the

Received: November 8, 2016
Revised: January 19, 2017
Accepted: January 20, 2017
Published: January 20, 2017

DOI: 10.1021/acs.iecr.6b04350
Ind. Eng. Chem. Res. 2017, 56, 1416−1423

partial destruction of the network and consequently originating a mesopore system.[10,12,17]

Simple laboratory experiments with sequential reaction systems can provide useful information about the relative magnitude of diffusion phenomena, provided the data analysis is correct, without the need for further experiments or complex determinations.[14] For example, it was shown that in the conversion of 1,3,5-tri-isopropylbenzene (TIPB, critical diameter 9.5 Å) over FCC catalysts prepared with Y zeolite with various degrees of intracrystalline mesoporosity, the new pore systems improved not only the observed catalyst activity (higher conversion) but also the selectivity to the primary cracking product (1,3-di-isopropylbenzene, critical diameter 8.4 Å).[12] Martínez et al.[8] used USY zeolites modified with NaOH and EDTA, which were further stabilized, in the cracking of vacuum gas oil; they observed that besides showing a higher activity than the parent zeolite, the modified catalysts showed a higher selectivity to LCO, considered an intermediate product in the FCC conversion mechanism of VGO (Scheme 1).[8,17] In

Scheme 1. Simplified FCC VGO Conversion Mechanism

$$VGO \rightarrow LCO \rightarrow gasoline, gases.$$

both cases this is the consequence of the faster diffusion of the primary products out of the catalyst pore system which, consequently, are not seriously involved in additional cracking reactions.

n-Hexadecane (*n*-C_{16}, molecular weight 226 g/g mol) has been used as a model reactant representative of paraffinic feedstocks to study various FCC issues.[18−21] Among different advantages (high boiling point liquid, ease of handling, etc.), products from hexadecane conversion are very much the same as those with less than 16 carbon atoms from VGO conversion. Differently from TIPB, where sequential steps of scission of the side alkyl chains can be defined[9,12] and the aromatic products from primary (1,3-di-isopropylbenzene) and secondary (cumene and benzene) cracking can be unequivocally identified, the analysis of primary and secondary cracking products in the conversion of C_{16} is not as direct. For example, if among the products of C_{16} cracking a paraffin with six carbon atoms per molecule (C_6) is apparent, it cannot be determined if it was produced by the scission of a C−C bond in a C_{16} reactant molecule, an event which would also produce a C_{10} molecule, or if it was produced from molecules which were in turn the product of previous cracking events.

Tauster and co-workers[14] developed a method to assess diffusional inhibitions via the analysis of sequential ($A \rightarrow B \rightarrow C$) reactions despite the lack of formal "*B*" and "*C*" molecules. They developed the primary and secondary cracking analysis (PASCA) based on a simple balance of carbon atoms among the products of the hydrocracking of 3-methylpentane over a Pt−Ir/γ-Al_2O_3 catalyst with two particle sizes and found that the larger the particles the more extended the secondary cracking as compared to primary cracking, as the consequence of more severe diffusion restrictions.

It is the objective of this work to confirm that the PASCA methodology can be successfully applied to the analysis of the product distribution of *n*-hexadecane cracking under conditions close to those in the commercial FCC process over both catalyst prototypes including Y zeolite with different degrees of intracrystalline mesoporosity and equilibrium commercial catalysts. The improvements in the diffusion of primary hydrocarbon products induced by the modified textural properties of the zeolite could be consequently characterized.

2. PRIMARY AND SECONDARY CRACKING ANALYSIS (PASCA)

Considering that the coke yield in the experiments of conversion of C_{16} can be neglected (see section 4, Results and Discussion), the PASCA method developed by Tauster et al.[14] will be adapted to this particular case. For a given mass of reactant fed to the reactor (all calculations in this work are referred to a mass basis of 100 g of reactant), the number of moles of product molecules produced by the cracking of C_{16} (n_{C1-15}) is

$$n_{C1-15} = \sum_{i=1}^{15} n_{Ci} \tag{1}$$

where C_i are all compounds with *i* carbon atoms per molecule, independently from their chemical nature, and n_{Ci} are the moles of molecules of the corresponding C_i compounds.

In the catalytic conversion of *n*-C_{16} it is common to observe C_{16} isomers besides the cracking products, which are added to the pure reactant to conform a single entity.

In turn, the number of moles of carbon atoms which are included in the products from C_{16} cracking is

$$a_{C1-15} = \sum_{i=1}^{15} i n_{Ci} \tag{2}$$

Thus, the average number of carbon atoms per molecule in the cracking products can be calculated as

$$\mu = \frac{a_{C1-15}}{n_{C1-15}} \tag{3}$$

The cracking of C_{16} (primary cracking) increases both n_{C1-15} and a_{C1-15}, but the cracking of any of those products (secondary cracking) will only produce an increase in n_{C1-15}, while a_{C1-15} will remain unaltered. If only primary cracking occurs, that is, if only C_{16} reacts while the product molecules do not crack again

$$\frac{n_{C1}}{n_{C15}} = \frac{n_{C2}}{n_{C14}} = \frac{n_{C3}}{n_{C13}} = \ldots = \frac{n_{Ci}}{n_{C(16-i)}} = \ldots = 1 \tag{4}$$

It is simple then to show that the average number of carbon atoms per molecule in the products when only primary cracking occurs (μ^{OPC}) is

$$\mu^{OPC} = 8 \tag{5}$$

and the number of moles of carbon atoms in the cracking products (see eq 3) is

$$a_{C1-15} = 8 n^{OPC}_{C1-15} \tag{6}$$

where n^{OPC}_{C1-15} is the number of moles of product molecules when only primary cracking occurs.

When a C_{16} molecule is cracked, two (if only primary cracking occurs) or more (if secondary cracking occurs) product molecules are generated. Moreover, independently of the occurrence of secondary cracking, the total number of carbon atoms in the cracking products, per each C_{16} molecule cracked, is 16. Thereby, the extension of the primary cracking (A_{PC}) can be defined as the amount of C_{16} molecules cracked, that is

DOI: 10.1021/acs.iecr.6b04350
Ind. Eng. Chem. Res. 2017, 56, 1416−1423

$$A_{PC} = \frac{a_{C1-15}}{16} = n_{C1-15}\frac{\mu}{16} \quad (7)$$

Similarly, the extension of the secondary cracking (A_{SC}) is the total amount of product molecules minus the amount of molecules produced only by the primary cracking, that is

$$A_{SC} = n_{C1-15} - n_{C1-15}^{OPC} \quad (8)$$

By considering eq 6 it results

$$A_{SC} = n_{C1-15} - \frac{a_{C1-15}}{8} \quad (9)$$

which after eq 3 is

$$A_{SC} = n_{C1-15}\left(1 - \frac{\mu}{8}\right) \quad (10)$$

Finally, the relationship between secondary and primary cracking (A_{SC}/A_{PC}) is (see eqs 10 and 7)

$$\frac{A_{SC}}{A_{PC}} = \frac{16}{\mu} - 2 \quad (11)$$

Equation 11 quantifies the relative incidence of the secondary cracking reactions as compared to those of primary cracking by means of a simple expression which only depends on the average number of carbon atoms in the C_{16} cracking products (μ). The analysis of results following this straightforward methodology can help in the assessment of the incidence of diffusion restrictions,[14] given the fact that conversion schemes with consecutive overall reactions like this ($A \rightarrow B \rightarrow C$) will show a higher incidence of secondary cracking reactions where the diffusion of intermediate products is hindered.[8,11−14]

The basic concept is simple: if only the cracking reaction of the reactant takes place, equal amounts of the corresponding fragments are expected (see eq 4); if secondary cracking takes place, the proportion of larger fragments will decrease and that of the smaller fragments increases accordingly. Consequently, the average number of carbon atoms among the cracking products will be smaller and A_{SC}/A_{PC} (Equation 11) will increase. Thus, this relationship is a tool which would allow characterizing the catalytic performance of FCC catalysts under conditions close to those of the commercial process, given the previous considerations. One of the clear advantages is that only a few undemanding experiments and the observed product distributions are required.

3. EXPERIMENTAL SECTION

Two prototypes of FCC catalysts were used in the experiments of conversion of n-C_{16}. One of them was prepared with a Y zeolite where intracrystalline mesoporosity was induced by means of an alkaline leaching procedure.[10−12] A portion of a commercial Y zeolite (Zeolyst CBV 760, Si/Al = 30, H-form) was immersed in a 0.10 M NaOH aqueous solution at 1 g zeolite/30 mL and kept under stirring at 25 °C for 15 min. After that the suspension was neutralized with a HCl 1.00 M solution. This zeolite was exchanged three times with a 0.50 M NH_4Cl (Carlo Erba, 99.5%) solution at 1 g zeolite/5 mL and then thoroughly washed with deionized water, dried for 16 h at 110 °C, and finally calcined during 4 h at 550 °C. The zeolite was named Z-10. A second catalyst was prepared using the parent zeolite (no treatment), which was named Z-00.

The zeolites were characterized by various techniques. The textural properties were assessed after the adsorption of nitrogen at −196 °C in a Quantachrome Autosorb-1 sorptometer, the samples being previously degassed at 300 °C during 3 h. The BET method was used to determine the specific surface area using the $0.15 < P/P_o < 0.30$ range, the total pore volume was estimated at $P/P_o \approx 0.98$, and the micropore volume and the specific surface area of the mesopores were estimated with the t-plot method in the 3.5 Å $< t <$ 5.0 Å range. The Barrett−Joyner−Halenda (BJH) model was used to determine the mesopore size distribution and the average pore diameter. A Shimadzu XD-D1 diffractometer was used to collect the zeolite X-ray diffraction patterns in the $5° < 2\theta < 40°$ range. The unit cell sizes (UCS) were calculated following the ASTM D 3942 method, and the crystallinity was determined with the ASTM D 3906 method. The amount, nature, and strength of the acidic sites in the zeolites were determined with the FTIR analysis of adsorbed pyridine (Merck, 99.5%) in a Shimadzu FTIR Prestige-21 spectrophotometer. Self-supporting wafers with a density of 440 g/m^2 were conformed with approximately 100 mg of the zeolites, which were located in a cell with CaF_2 windows. A background spectrum was collected at room temperature with samples degassed at 10^{-4} Torr and 450 °C for 2 h. Pyridine adsorption was performed at room temperature, and successive desorptions were produced at 150, 300, and 400 °C. The spectra were recorded at room temperature with a resolution of 4 cm^{-1}. The amounts of Brönsted and Lewis acid sites were calculated based on the integrated absorbance of the bands at 1545 and 1450−1460 cm^{-1}, respectively.[22]

Both the parent and the desilicated zeolite samples were steamed (100% steam) at 788 °C for 5 h in order to stabilize them. The prototypes of FCC catalysts were prepared by mixing the stabilized zeolites with an essentially inactive matrix (Merck, Silica gel 60, code number 107734) and a colloidal silica binder (Ludox AS-40, Aldrich).[11,12] The zeolite, matrix, and binder were added at 30, 50, and 20 wt %, respectively, reproducing typical formulations of the commercial FCC catalysts.[2,9] Then the catalysts were dried for 16 h at 110 °C and calcined in an oven for 4 h at 550 °C in air. Finally, the catalysts were grounded and sieved to the 75−125 μm size range. The resulting particles had an average bulk density of 0.87 g/cm^3, which is similar to those in commercial catalysts (0.80−0.96 g/cm^3) and permits the correct fluidization of the catalyst.[23] The catalysts were designated as Cat-00 and Cat-10, according to the nomenclature of the corresponding zeolites.

The experiments of n-C_{16} (Alfa Aesar, >99%) catalytic conversion were performed in a CREC Riser Simulator reactor, which is a batch fluidized bed laboratory reactor which closely mimics the conditions of the commercial FCC process. In that sense, the ranges of reaction temperatures, catalyst to oil relationships, and, more importantly, reaction times in the order of a few seconds should be regarded.[24] The unit has been described comprehensively elsewhere.[9,19,20,24] The reaction time in the experiments was 4 s, temperatures were 500 and 550 °C, and the catalyst to oil relationship was 2.6, achieved with a mass of catalyst of 0.4 g in all cases. The reaction products were analyzed by online standard capillary gas chromatography using a 30 m long, 250 μm diameter, and 0.25 μm film thickness, nonpolar, dimethylpolysiloxane column. Product identification was performed with the help of standards, GC-MS, and IR spectroscopy. The coke content on the catalyst was assessed by means of a temperature-programmed oxidation method and further methanation of the carbon oxides over a Ni catalyst, quantified with the help of a

DOI: 10.1021/acs.iecr.6b04350
Ind. Eng. Chem. Res. 2017, 56, 1416−1423

FID detector. Mass balances (recoveries) were close to more than 90% in all cases.

4. RESULTS AND DISCUSSION

The properties of both the raw zeolite (Z-00) and the desilicated sample (Z-10) are shown in Table 1 together with the corresponding steamed samples (Z-00-S and Z-10-S, respectively). Figure 1 shows the mesopore size distribution for both parent and desilicated zeolites. A more detailed discussion about the Y zeolite desilication process and its impact on the zeolite properties, which are out of the scope of this work, can be found in various references.[8,10−12,17] However, the catalytic performance of the samples will be analyzed in relation to these properties.

Table 1. Properties of the Parent and Desilicated Zeolites before and after Steaming

	Z-00	Z-10	Z-00-S	Z-10-S
textural properties				
BET specific surface area (m^2/g)	838	828	681	639
micropore specific surface area[a] (m^2/g)	612	462	570	467
mesopore specific surface area (m^2/g)	226	366	111	172
total pore volume (cm^3/g)	0.632	0.686	0.515	0.585
micropore volume (cm^3/g)	0.350	0.266	0.242	0.197
mesopore volume[b] (cm^3/g)	0.282	0.420	0.273	0.388
average mesopore diameter (Å)	28.7	44.2	61.8	65.0
crystalline properties				
crystallinity (%)	100[c]	66	95	29
unit cell size (Å)	24.23	24.25	24.24	24.21
acidic properties				
Bronsted acidity (μmol Py/g)				
T_{des} = 150 °C	60	126	2	9
T_{des} = 300 °C	53	83	1	2
T_{des} = 400 °C	21	30	1	2
Lewis acidity (μ_{mol} Py/g)				
T_{des} = 150 °C	23	49	29	31
T_{des} = 300 °C	15	40	17	32
T_{des} = 400 °C	16	27	14	8

[a]Micropore surface area = BET specific surface area − mesopore surface area. [b]Mesopore volume = total pore volume − micropore volume. [c]Reference sample.

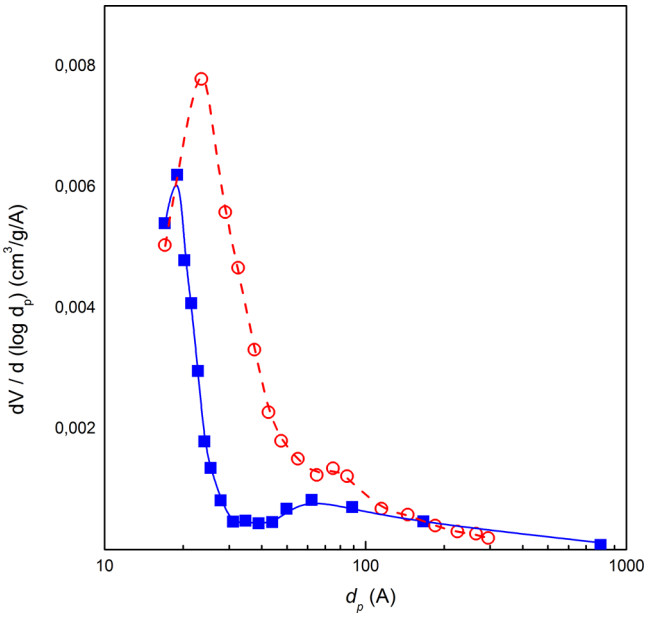

Figure 1. Mesopore size distributions (BJH) of the parent and desilicated zeolites: (blue squares) Z-00; (red circles) Z-10.

It can be seen in Table 1 and Figure 1 that the parent zeolite Z-00 had mesopores, particularly in the 20−30 Å size range (average mesopore diameter 28.7 Å), contributing 226 m^2/g to the specific surface area. The modified zeolite Z-10 had a mesopore specific surface area two times that of the parent zeolite, the average mesopore diameter was 44.2 Å, and the mesopore volume increased about 50% after alkaline leaching.

The X-ray diffraction patterns (not shown) showed that the intensity of most of the peaks in the treated sample decreased, showing 66% crystallinity.[12] Similar results in relation to the loss of crystallinity in the same Y zeolite (CBV 760) after alkaline lixiviation were reported by Verboekend et al.,[25] which are attributed to partial destruction of the framework due to the removal of Si atoms.[10,25] The slight increase in UCS is the consequence of that selective silicon extraction, since the length of Si−O bonds in the zeolite framework is shorter than that of the Al−O bonds, thus producing a larger size of the unit cell.[5,25]

The amount of acidic sites in the zeolite (on a mass basis) increased after the alkaline leaching and ion exchange steps. The effect was observed both on total acidity (as shown by the lowest desorption temperature 150 °C) and on each range of acid strength. It had been shown that the lixiviation process is highly selective to leaching out silica-rich domains.[10,25] Conversely, aluminum-rich domains and, consequently, tetrahedral Al atoms would remain relatively unchanged in the crystalline material, thus producing an increase in acidity on a mass basis.

Steaming the zeolites lead to expected results, that is, it produced loss of crystallinity and specific surface area, which was more intense on the desilicated sample. However, all properties (average mesopore size, specific surface area, crystallinity, acidity) maintained the trends observed with the zeolites before steaming. Similar results had been reported by Martínez et al.[8,17] after steaming Y zeolites treated with NaOH and EDTA.

Table 2 shows an example of a typical product distribution (case of catalyst Cat-00, 500 °C) in the cracking of *n*-C_{16}. The products included represent more than 97 wt % of the hydrocarbons in the gas phase, the rest being minor products, with individual yields lower than 0.02 wt %. The yield of coke was negligible in all cases (coke on catalyst in the range of 0.11−0.16 wt %).

It must be considered in the analysis of product distributions that, according to well-known mechanisms,[26] in simplified terms, the catalytic cracking of a paraffin leads to the production of a paraffin and an olefin of smaller molecular size. However, in the parent work by Tauster et al.,[14] in the hydrocracking of a C_6 hydrocarbon over bifunctional (Pt−Ir/Al_2O_3) catalysts, the olefins produced in each cracking step on the acidic function can be later hydrogenated on the metallic function, leading to a much higher proportion of paraffins among the products. The experimental data of conversion of *n*-C_{16} produced C_{16} isomers and lighter products can be seen in Table 2. Moreover, for the example shown, among the C_{1-15} products *n*-paraffins represented more than 70 wt %, olefins about 21.5 wt %, *i*-praffins about 3.5 wt %, and, to a lower

DOI: 10.1021/acs.iecr.6b04350
Ind. Eng. Chem. Res. 2017, 56, 1416−1423

Table 2. Product Distribution in the Cracking of n-C_{16} over Catalyst Cat-00 at 500 °C (4 s, Cat/Oil 2.6)[a]

	mass fraction (wt %)		mass fraction (wt %)
C_1	0.13	3-$C_7^=$	0.02
C_2 + $C_2^=$	1.14	n-C_7	0.51
C_3 + $C_3^=$	0.92	c-2-$C_7^=$	0.05
i-C_4	0.21	1-$C_8^=$	0.03
n-C_4	0.77	DiMeCyC$_6$	0.09
t-$C_4^=$	0.03	n-C_8	0.49
c-$C_4^=$	0.03	t-2-$C_8^=$	0.07
i-C_5	0.14	3-MeC$_8$	0.03
1-$C_5^=$	0.25	$C_9^=$	0.16
n-C_5	0.58	n-C_9	0.46
t-$C_5^=$	0.02	1-$C_{10}^=$	0.08
$C_5^{==}$	0.07	n-C_{10}	0.47
2-Me2-$C_4^=$	0.04	n-C_{11}	0.49
4-Me1-$C_5^=$	0.02	1,2,4-TriEtBz	0.05
$C_6^{==}$	0.16	n-C_{12}	0.47
n-C_6	0.69	n-C_{13}	0.51
3-$C_6^=$	0.02	n-C_{14}	0.45
2-Me2-$C_5^=$	0.05	n-C_{15}	0.17
MeCyC$_5$	0.02	C_{16} isomers	6.94
2-MeC$_6$	0.02	n-C_{16}	80.32

[a] i, iso; n, normal; t, trans; c, cis; Me, methyl; Et, ethyl; Cy, cycle; Bz, benzene.

extent, naphthenic and aromatic compounds about 1.1 and 0.5 wt %, respectively.

As already mentioned, the more severe the diffusion restrictions on the intermediate product B in sequential reactions of the type $A \rightarrow B \rightarrow C$ (the more extended the contact time inside the pore system), the more significant its conversion to product C and the lower the B selectivity.[12−14] Changes of the relative importance of secondary cracking as a consequence of more important diffusion restrictions in given catalysts can be assessed by means of kinetic models. For example, a simple pseudohomogeneous model considering first-order reactions in the primary and secondary cracking was applied to describe the conversion of 1,3,5-tri-isopropylbenzene (critical diameter 9.5 Å) over zeolites with different crystalline mesoporosity, defining a "secondary cracking index" as the relationship between the apparent kinetic constants of the secondary and primary cracking reactions.[12] It was shown that the higher the mesoporosity, the less severe the diffusion restrictions, the shorter the residence time in the pores, and the lower the index.[12,27] Various paraffins have been extensively used as model reactants to study different aspects in FCC, such as product selectivities, magnitude of hydrogen transfer reactions, relative importance of cracking mechanisms, and degree of product olefinicity.[18−21] However, if a paraffin such as n-hexadecane is to be used in the kinetic analysis of sequential $A \rightarrow B \rightarrow C$ reactions, a direct approach is not possible due to the lack of formal "B" and "C" molecules.

It was previously shown that if only primary cracking of C_{16} occurs (the product C_{1-15} molecules do not crack), the $n_{Ci}/n_{C(16-i)}$ relationship should be equal to one (eq 4); on the contrary, if secondary cracking occurs up to a certain extension (C_{1-15} molecules crack), the relationship will be higher than one, with i lower than 8. Table 3 shows the $n_{Ci}/n_{C(16-i)}$ molar relationships for the various products observed in experiments at 500 and 550 °C over both catalysts. It can be seen in all cases that the $n_{Ci}/n_{C(16-i)}$ relationships (with $i < 8$) were larger than

Table 3. Relationships between Molar Selectivities ($n_{Ci}/n_{C(16-i)}$) in the Products of n-C_{16} Cracking over Catalysts Cat-00 and Cat-10 (4 s, Cat/Oil 2.6)

	Cat-00		Cat-10	
	500 °C	550 °C	500 °C	550 °C
n_{C1}/n_{C15}	10.07	26.42	7.44	21.28
n_{C2}/n_{C14}	13.50	24.11	11.99	24.33
n_{C3}/n_{C13}	4.27	7.00	4.28	6.98
n_{C4}/n_{C12}	4.88	4.67	4.59	5.98
n_{C5}/n_{C11}	2.72	2.72	2.07	3.15
n_{C6}/n_{C10}	1.92	2.15	1.60	2.03
n_{C7}/n_{C9}	1.50	1.51	1.38	1.41

one, thus being evidence of the existence of secondary cracking, which is certainly an expected fact. It can be noted that except for n_{C1}/n_{C15}, the smaller the i index the higher the relationship. This can be understood considering that molecules (for example, C_6) can be formed as the consequence of primary C_{16} cracking (also producing a C_{10} molecule) but can also be formed from cracking reactions from other molecules (C_7, C_8, ..., C_{14}, C_{15}), the effect being more notorious when the molecular size considered is smaller.

It can also be noted that the n_{C1}/n_{C15} relationship does not obey the same trend. This can be rationalized in the light that after an initiation step where both monomolecular (protolytic, carbonium ion) and bimolecular (carbenium ion) cracking mechanisms coexist, conventional β-scission cracking prevails.[19] Thus, the smaller product molecule would be C_2, while methane could be produced by either protolytic or thermal cracking, both options being favored at higher temperatures.[19] This view is supported by the fact that the selectivity to methane (C_1) was 0.67 wt % with Cat-00 and 0.50 wt % with Cat-10 in the experiments at 500 °C and increased more than twice in the experiments at 550 °C (1.44 wt % with Cat-00 and 1.29 wt % with Cat-10).

The PASCA method allows determining the relationship between the extension of secondary and primary cracking (A_{SC}/A_{PC}, eq 11) once the average number of carbon atoms in the product molecules (μ, eq 3) is known. The relationship A_{SC}/A_{PC} is closely related to the diffusion restrictions imposed by the catalyst pore system on the reaction products. Table 4 shows the main parameters of the PASCA analysis in the catalytic cracking of n-C_{16} over both catalysts at 500 and 550 °C. It can be seen with both catalysts that, as expected, the activity increased with the reaction temperature. Moreover, at both temperatures, the catalyst whose zeolite had more

Table 4. Primary and Secondary Cracking Analysis in the Catalytic Cracking of n-C_{16} over Catalysts Cat-00 and Cat-10 (4 s, Cat/Oil 2.6)[a]

	Cat-00		Cat-10	
	500 °C	550 °C	500 °C	550 °C
$X_{n\text{-}C16}$	19.7	21.9	20.4	29.7
n_{C1-15}	0.171	0.248	0.174	0.347
α_{C1-15}	0.903	1.123	0.953	1.623
μ	5.27	4.53	5.49	4.67
A_{PC}	0.056	0.070	0.060	0.101
A_{SC}	0.058	0.107	0.055	0.145
A_{SC}/A_{PC}	1.035	1.529	0.917	1.426

[a] On the basis of 100 g of n-C_{16} reactant.

DOI: 10.1021/acs.iecr.6b04350
Ind. Eng. Chem. Res. 2017, 56, 1416−1423

mesopores (Cat-10) was more active than the parent one (Cat-00). This behavior was also observed for the same catalysts in the conversion of 1,3,5-tri-isopropylbenzene[12] and in the catalytic upgrading of bio-oil from pine sawdust.[11] The higher observed activity in catalyst Cat-10 can be attributed to the combined effect of its higher intracrystalline mesoporosity, which permits an improved transport of reactant molecules to the active sites, and to its higher density of acidic sites, which catalyze cracking reactions. Additionally, the positive effect of improved diffusion properties on the observed activity was confirmed in the conversion of 1,3,5-tri-isopropylbenzene over two catalysts which had similar acidities but differed in the amount of intracrystalline mesoporosity, where the catalyst with the higher mesoporosity was the most active in the cracking of that bulky molecule.[12]

The values of n_{C1-15}, a_{C1-15}, μ, A_{PC}, A_{SC}, and A_{SC}/A_{PC} in Table 4 were calculated by means of eqs 1, 2, 3, 7, 9, and 11, respectively. As expected, the amount of product molecules (n_{C1-15}) and the extension of primary cracking (A_{PC}) are consistent with the conversions observed. At both reaction temperatures the average number of carbon atoms in the cracking product molecules (μ) was higher in the catalyst whose zeolite had a larger intracrystalline mesoporosity (Cat-10). This is consistent with the previous discussion about results in Table 3 since, in general terms for a given i number, the $n_{Ci}/n_{C(16-i)}$ relationship observed with catalyst Cat-10 was lower than that with catalyst Cat-00.

The higher reaction temperature induced a more important relative incidence of secondary cracking (larger A_{SC}/A_{PC} values). This is consistent with published results,[12,14,19] which attribute this behavior to the more significant positive impact of temperature on chemical reaction kinetics than on diffusion processes. Consequently, the diffusion control would be more important, and the secondary cracking reactions will be more predominant.

It can be seen in Table 4 when the conversion of n-C_{16} was carried out at 550 °C that the extension of the secondary cracking (A_{SC}) in catalyst Cat-10 was larger than that observed with Cat-00 (0.145 vs 0.107). Nevertheless, the extension of the primary cracking (A_{PC}) increased more (0.101 vs 0.070, respectively). Thus, results shown in Table 4 demonstrate that increasing the intracrystalline mesoporosity in Y zeolite decreases the relative incidence of secondary cracking as compared to primary cracking (A_{SC}/A_{PC}). This positive effect is the consequence of the improvement in the diffusion transport of reactant molecules, which is diffusing faster out of the zeolite pore system and has fewer chances to be subjected to further cracking. This effect seems to overwhelm the higher acidity of zeolite Z-10 in comparison with that of the parent zeolite (Z-00), since the higher density of acidic sites would support more activity and, consequently, a more extended development of consecutive reactions.

According to eq 11, the relationship A_{SC}/A_{PC} is theoretically restricted to the 0−14 range. In effect, the maximum possible value for the average number of carbon atoms per molecule in the C_{16} cracking products is $\mu = 8$, corresponding to the case where only primary cracking occurs ($\mu = \mu^{OPC}$), which leads to $A_{SC}/A_{PC} = 0$. The other extreme situation is that in which all intermediate products cracked as much as possible, causing methane to be the only product, with $\mu = 1$. These are completely theoretical, unfeasible situations. Therefore, it is interesting to compare the values of A_{SC}/A_{PC} corresponding to these prototype catalysts with those observed in equilibrium commercial FCC catalysts, that is, actual catalysts from running refineries. Figure 2 shows the A_{SC}/A_{PC} relationships observed as a function of conversion in the catalytic cracking of n-C_{16} at various temperatures over two equilibrium commercial FCC catalysts. The information was gathered in previous experiments in the same reactor[19] using E-Cat-O (BET specific surface area 151 m^2/g, zeolite content 15.9 wt % (unit cell size 24.24 Å, free of rare earths)) and E-Cat-E (BET specific surface area 147 m^2/g, zeolite content 11.5 wt % (unit cell size 24.29 Å, rare-earth content: 1.42 wt %)). Even though equilibrium commercial catalysts are more complex than laboratory prototypes in the sense that they surely include contaminant metals and possibly additives of specific function, besides that the matrix can be active itself, the PASCA method, based on a simple mass balance of the carbon atoms among products, would still be applicable.

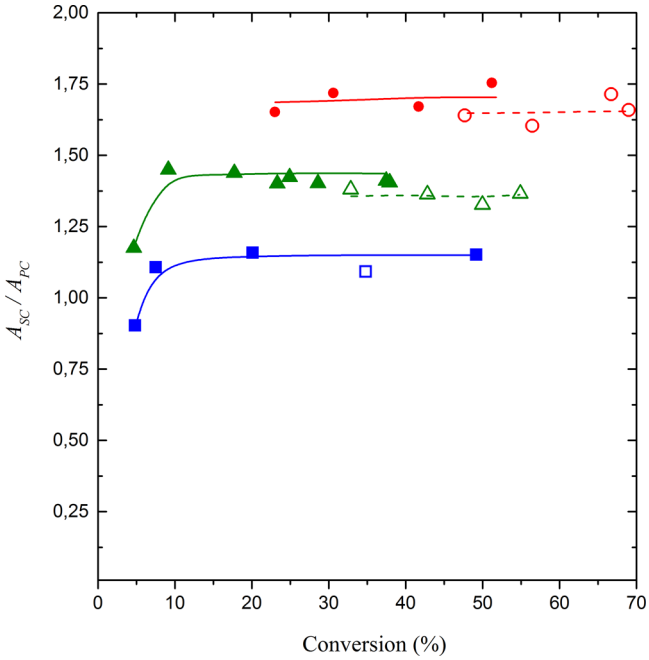

Figure 2. A_{SC}/A_{PC} relationship as a function of conversion in the cracking of n-C_{16} over equilibrium commercial catalysts at various temperatures. Symbols: open, E-Cat-O; closed, E-Cat-E. Temperatures: 440 (blue squares), 500 (green triangles), and 550 °C (red circles).

As it can be observed in Figure 2, at low conversion, A_{SC}/A_{PC} increases as a function of conversion. This is consistent with the fact that at low conversion the amount of cracking products (n_{C1-15}) is small as compared to the amount of unconverted reactant; thus, the occurrence of secondary cracking is much reduced and, in the limit, $A_{SC}/A_{PC} \rightarrow 0$. As conversion increases, n_{C1-15} and the occurrence of secondary cracking increase and consequently so does A_{SC}/A_{PC}. Regardless of the catalyst and reaction temperature, when conversion is higher than approximately 10%, the A_{SC}/A_{PC} profile becomes essentially stable, independent of conversion. At conversions close to 100%, the amount of unconverted reactant will be negligible and the coke yield probably should not be disregarded in the balances. However, it is certainly possible to expect that the A_{SC}/A_{PC} relationship would increase significantly.

DOI: 10.1021/acs.iecr.6b04350
Ind. Eng. Chem. Res. 2017, 56, 1416−1423

In accordance with the previous observations about the impact of reaction temperature on A_{SC}/A_{PC} (see Table 4), it can be seen in Figure 2 that the higher the temperature the higher the A_{SC}/A_{PC}, given the more significant effect on chemical reaction kinetics. Moreover, the secondary to primary cracking relationships observed in commercial catalysts are in the same range as those for the laboratory prototypes, though slightly higher. At a given reaction temperature, for example, 500 °C, the relationships follow the order Cat-10 < Cat-00 < E-Cat-O < E-Cat-E from 0.917 to 1.438 (the same ranking was observed at 550 °C). The slightly higher values of equilibrium commercial catalysts could be understood as the consequence of some activity in their matrices, as differently from the prototypes.

5. CONCLUSIONS

The method of primary and secondary cracking analysis (PASCA) was successfully applied to the analysis of the product distributions of the n-C_{16} cracking, under conditions close to those in the commercial FCC process, over prototypes of FCC catalysts with Y zeolites having different degrees of intracrystalline mesoporosity.

The experiments of conversion of n-C_{16}, performed in a CREC Riser Simulator reactor, showed that the increased intracrystalline mesoporosity (induced by alkaline desilication) in the Y zeolite crystals decreases the relative incidence of secondary cracking reactions as compared to those of primary cracking (A_{SC}/A_{PC}), thus increasing the selectivity to intermediate products. That positive effect is the consequence of improvements in the diffusion transport of intermediate product molecules which, in diffusing faster out of the zeolite pore system, are less prone to secondary reactions.

This approach can also be applied to the evaluation of commercial catalysts. The experiments performed with equilibrium commercial catalysts exhibited similar, though slightly higher, values of A_{SC}/A_{PC} in comparison with the prototypes prepared in the laboratory. In all cases the relationship increased at higher reaction temperatures, thus showing the impact of this parameter which was stronger on chemical reaction kinetics than on the transport diffusion processes.

The PASCA analysis, which only needs to know the product distributions in straightforward cracking experiments, was shown to be a useful tool to evaluate the occurrence of diffusion restrictions under reaction conditions and its impact on product selectivities, without the need for complex assessments of parameters. The approach is particularly applicable to the comparison of catalysts in a series of samples subjected to, e.g., different synthesis conditions or modifications or to evaluation of the impact of the operation conditions for given catalysts.

AUTHOR INFORMATION

Corresponding Author

*Tel.: +54 (342) 451-1370 ext 6102. E-mail: usedran@fiq.unl.edu.ar.

ORCID

Ulises Sedran: 0000-0002-4145-2834

Notes

The authors declare no competing financial interest.

ACKNOWLEDGMENTS

The financial support of the Universidad Nacional del Litoral (Project CAID 2011 #50120110100546) and CONICET (PIP 593/13) is gratefully acknowledged.

REFERENCES

(1) O'Connor, P. Catalytic Cracking: The Future of an Evolving Process. *Stud. Surf. Sci. Catal.* **2007**, *166*, 227−251.

(2) Komvokis, V.; Tan, L.; Clough, M.; Pan, S.; Yilmaz, B. Zeolites in Catalytic Cracking (FCC). In *Zeolites in Sustainable Chemistry. Synthesis, Characterization, and Catalytic Applications*; Xiao, F., Meng, X., Eds.; Springer: Heidelberg, 2016; pp 271−297.

(3) Jiménez-García, G.; Aguilar-López, R.; Maya-Yescas, R. The Fluidized-Bed Catalytic Cracking Unit Building its Future Environment. *Fuel* **2011**, *90*, 3531−3541.

(4) Letzsch, W.; Ashton, A. The Effect of Feedstock on Yields and Product Quality. *Stud. Surf. Sci. Catal.* **1993**, *76*, 441−498.

(5) Scherzer, J. Octane-Enhancing, Zeolite FCC Catalysts: Scientific and Technical Aspects. *Catal. Rev.: Sci. Eng.* **1989**, *31*, 215−354.

(6) García-Martínez, J.; Li, K.; Krishnaiah, G. A Mesostructured Y Zeolite as a Superior FCC Catalyst − from Lab to Refinery. *Chem. Commun.* **2012**, *48*, 11841−11843.

(7) Prasomsri, T.; Jiao, W.; Weng, S.; García-Martínez, J. Mesostructured Zeolites: Bridging the Gap Between Zeolites and MCM-41. *Chem. Commun.* **2015**, *51*, 8900−8911.

(8) Martinez, C.; Verboekend, D.; Pérez-Ramírez, J.; Corma, A. Stabilized Hierarchical USY Zeolite Catalysts for Simultaneous Increase in Diesel and LPG Olefinicity During Catalytic Cracking. *Catal. Sci. Technol.* **2013**, *3*, 972−981.

(9) Al-Khattaf, S.; de Lasa, H. The Role of Diffusion in Alkylbenzenes Catalytic Cracking. *Appl. Catal., A* **2002**, *226*, 139−153.

(10) Na, K.; Choi, M.; Ryoo, R. Recent Advances in the Synthesis of Hierarchically Nanoporous Zeolites. *Microporous Mesoporous Mater.* **2013**, *166*, 3−19.

(11) García, J. R.; Bertero, M.; Falco, M.; Sedran, U. Catalytic Cracking of Bio-oils Improved by the Formation of Mesopores by Means of Y Zeolite Desilication. *Appl. Catal., A* **2015**, *503*, 1−8.

(12) García, J. R.; Falco, M.; Sedran, U. Impact of the Desilication Treatment of Y Zeolite on the Catalytic Cracking of Bulky Hydrocarbon Molecules. *Top. Catal.* **2016**, *59*, 268−277.

(13) Wheeler, A. Reaction Rates and Selectivity in Catalyst Pores. *Adv. Catal.* **1951**, *3*, 249−327.

(14) Tauster, S.; Ho, T.; Fung, S. Assessment of Diffusional Inhibition via Primary and Secondary. *J. Catal.* **1987**, *106*, 105−110.

(15) Farcasiu, M.; Degnan, T. The Role of External Surface Activity in the Effectiveness of Zeolites. *Ind. Eng. Chem. Res.* **1988**, *27*, 45−47.

(16) Li, K.; Beaver, M.; Speronello, B.; García-Martínez, J. Surfactant-Templated Mesostructuring of Zeolites: From Discovery to Commercialization. In *Mesoporous zeolites. Preparation, Characterization and Applications*; García-Martínez, J., Li, K., Eds.; Wiley: Weinheim, 2015; pp 321−347.

(17) Li, K.; Valla, J.; García-Martínez, J. Realizing the Commercial Potential of Hierarchical Zeolites: New Opportunities in Catalytic Cracking. *ChemCatChem* **2014**, *6*, 46−66.

(18) Michalakos, P.; Robinson, R.; Tang, Y. Catalyst Deactivation in Cracking of Hexadecane and Commercial FCC Feed, Studied by Microactivity Test-Multiple Cold Trap (MAT-MCT) Technique. *Catal. Today* **1998**, *46*, 13−26.

(19) de la Puente, G.; Sedran, U. The Energy Gradient Selectivity Concept and the Routes of Paraffin Cracking in FCC Catalysts. *J. Catal.* **1998**, *179*, 36−42.

(20) Bidabehere, C.; Sedran, U. Simultaneous Diffusion, Adsorption, and Reaction in Fluid Catalytic Cracking Catalysts. *Ind. Eng. Chem. Res.* **2001**, *40*, 530−535.

(21) Jeon, H.; Park, S.; Woo, S. Evaluation of Vanadium Traps Occluded in Resid Fluidized Catalytic Cracking (RFCC) Catalyst for High Gasoline Yield. *Appl. Catal., A* **2006**, *306*, 1−7.

DOI: 10.1021/acs.iecr.6b04350
Ind. Eng. Chem. Res. 2017, 56, 1416−1423

(22) Emeis, C. Determination of Integrated Molar Extinction Coefficients for Infrared Absorption Bands of Pyridine Adsorbed on Solid Acid Catalysts. *J. Catal.* **1993**, *141*, 347−354.
(23) Chen, Y. Applications for Fluid Catalytic Cracking. In *Handbook of Fluidization and Fluid-particle Systems*; Yang, W., Ed.; Marcel Dekker, Inc., 2003; pp 384−401.
(24) de Lasa, H. US Patent 5.102.628, 1992.
(25) Verboekend, D.; Vilé, G.; Pérez-Ramírez, J. Mesopore Formation in USY and Beta Zeolites by Base Leaching: Selection Criteria and Optimization of Pore-Directing Agents. *Cryst. Growth Des.* **2012**, *12*, 3123−3132.
(26) Cumming, K.; Wojciechowski, B. Hydrogen Transfer, Coke Formation, and Catalyst Decay and Their Role in the Chain Mechanism of Catalytic Cracking. *Catal. Rev.: Sci. Eng.* **1996**, *38*, 101−157.
(27) Groen, J.; Zhu, W.; Brouwer, S.; Huynink, S.; Kapteijn, R.; Moulijn, J.; Pérez-Ramírez, J. Direct Demonstration of Enhanced Diffusion in Mesoporous ZSM-5 Zeolite Obtained via Controlled Desilication. *J. Am. Chem. Soc.* **2007**, *129*, 355−360.

DOI: 10.1021/acs.iecr.6b04350
Ind. Eng. Chem. Res. 2017, 56, 1416−1423